

Routes of photocatalytic destruction of chemical warfare agent simulants

Alexandre V. Vorontsov,^a Lev Davydov,^b Ettireddy P. Reddy,^b Claude Lion,^c Eugenii N. Savinov^a and Panagiotis G. Smirniotis^{*b}

^a Borekov Institute of Catalysis Novosibirsk 630090, Russia

^b Chemical Engineering Department, University of Cincinnati, Cincinnati, OH 45221-0171 USA.
E-mail: panagiotis.smirniotis@uc.edu

^c Institut de Topologie et de Dynamique des Systèmes de l'Université Paris-7 (CNRS UPRESA 7086), 1, rue Guy-de-la-Brosse, 75005 Paris, France

Received (in New Haven, CT, USA) 29th October 2001, Accepted 22nd January 2002

First published as an Advance Article on the web

Selected imitants of chemical warfare agents such as dimethyl methylphosphonate (DMMP), diethyl phosphoramidate (DEPA), pinacolyl methylphosphonate (PMP), butylaminoethanethiol (BAET) were subjected to photocatalytic and sonophotocatalytic treatment in aqueous suspensions of TiO_2 . Complete conversion of the same mass of imitants to inorganic products was obtained within 600 min for DMMP, DEPA, PMP, but required a longer time for BAET. Sonolysis accelerated photodegradation of DMMP. No degradation was observed without ultraviolet illumination. Final products of degradation were PO_4^{3-} , CO_2 for DMMP and PMP, PO_4^{3-} , NO_3^- (25%), NH_4^+ (75%), CO_2 for DEPA, and SO_4^{2-} , NH_4^+ , CO_2 for BAET. The number of main detected intermediate products increases in the order DMMP (7), DEPA (9), PMP (21), and exceeds 34 for BAET. Degradation of DMMP mainly proceeds through consecutive oxidation of methoxy groups and then the methyl group. Dimethyl hydroxymethylphosphonate and dimethylphosphate testify to the parallel oxidation of the methyl group. Destruction of DEPA mainly starts with cleavage of the P– NH_2 bond to form diethyl phosphate, which transforms further into ethyl phosphate. Oxidation of α and β carbons of ethoxy groups to form ethylphosphonoamidate, hydroxyethyl ethylphosphonoamidate and other products also contributes to the destruction. Photocatalytic degradation of PMP mainly starts with oxidation of the pinacolyl fragment, methylphosphonic acid and acetone being the major products. Oxidation of BAET begins with dark dimerization to disulfide, which undergoes oxidation of sulfur forming sulfinic and sulfonic acids as well as oxidation of carbons to form butanal, aminobutane, etc., and cyclic products such as 2-propylthiazole. A scheme of degradation was proposed for DMMP and DEPA, and starting routes for PMP and BAET. Quantum efficiencies of complete mineralization calculated as reaction rate to photon flux ratio approximate $10^{-3}\%$.

Chemical warfare agents (CWA) are the acting force of chemical weapons. International treaties prohibit further production of CWA and the existing stockpiles are to be irreversibly destroyed. Stockpiles of CWA as well as rockets, mines, bombs and projectiles containing CWA are currently destroyed by various techniques. In order to be destroyed, CWA and warheads usually have to be transported to the facilities. Transportation poses additional risk for accidents, especially in densely populated areas.

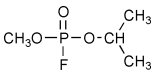
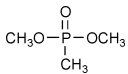
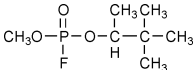
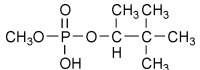
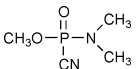
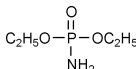
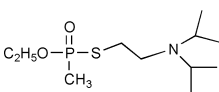
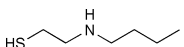
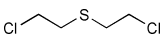
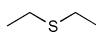
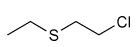
Besides incineration, which is commonly used in destruction of organics, there are several other prospective methods of destruction of CWA that are considered in short below.^{1–3} Formulas of common CWA are presented in Table 1. These molecules can be converted into less toxic species by nucleophilic substitution with hydroxyl anions or monoethanolamine ($\text{HOCH}_2\text{CH}_2\text{NH}_2$), destruction with aqueous hypochlorite or chlorine gas as well as with reagent oxone (mixture of KHSO_5 , KHSO_4 , and K_2SO_4), and peroxodisulfate ($\text{S}_2\text{O}_8^{2-}$). The recently developed reagent magnesium monoperoxophthalate affords complete detoxification of CWA under optimized conditions.³ The common disadvantage of neutralization reactions is that organic products have to be destructed further, either by incineration or by other methods. Oxidative reactions lead to complete mineralization of CWA; however, a big excess of

oxidizer is required. Biodegradation is another promising approach. It suffers, however, from slow rates and it cannot be applied directly to mustard gas, which destroys bacteria cells.

Photocatalytic destruction is promising as a one-step mineralization process for CWA. Complete mineralization by photocatalytic oxidation has been demonstrated for dimethyl methylphosphonate and diethyl methylphosphonate in the liquid^{4,5} and gas phases.⁶ Toxic pesticides such as methamidophos, malathion, diazinon, phorate,⁷ the insecticides dichlorvos and propoxur,⁸ the dye sulforhodamine B,⁹ which can also be considered as imitants of CWA, were mineralized in an illuminated suspension of TiO_2 . The drawback of photocatalysis is the same as for biodegradation: low rate of mineralization. Johnston and Hocking¹⁰ have demonstrated that ultrasonic irradiation of TiO_2 suspensions results in a marked increase of the photocatalytic degradation rate. We apply this approach to photocatalytic destruction of CWA simulants in aqueous suspension of TiO_2 as well.

The real CWA are deadly toxic liquids. Therefore, research on CWA is usually conducted with their less toxic structural analogs. We chose the least toxic compounds with chemical bonds characteristic of CWA (Table 1). Four of these simulants—dimethyl methylphosphonate (DMMP), pinacolyl

Table 1 Chemical warfare agents and chosen simulants

CWA formula	Simulant formula	Simulant properties		
		Molecular weight/g mol ⁻¹	Density/g cm ⁻³	Boiling point/°C
Sarin (GB) 	Dimethyl methylphosphonate (DMMP) 	124.08	1.161	180–181
Soman (GD) 	Pinacolyl methylphosphonate (PMP) 	180.19	1.032	96–106 at pressure 8 mm
Tabun (GA) 	Diethyl phosphoramidate (DEPA) 	153.12	–	140 at pressure 3 mm
VX 	2-(Butylamino)ethanethiol (BAET) 	133.26	0.901	112–115 at pressure 10 mm
Mustard gas or Yperite (HD) 	Diethyl sulfide (DES) 	90.19	0.835	92
	2-Chloroethyl ethylsulfide (CEES) 	124.63	1.070	156–157

methylphosphonate (PMP), diethyl phosphoramidate (DEPA), 2-(butylamino)ethanethiol (BAET)—are used in the current study as simulants for sarin, soman, tabun, and VX, respectively. The simulants for mustard gas in Table 1 were not used in this study because they are relatively volatile and are removed from the aqueous suspension during oxygen bubbling. However, their photocatalytic degradation is successfully performed in the gas phase.¹¹ DMMP possesses the P–C and P–O–C bonds met in GB and GD, whereas PMP has a structure identical to that of GD except that the fluorine atom of GD is substituted by an OH group. The P–F bond of GB and GD hydrolyses in water relatively quickly and even if we used real GD after a short period of time we would have PMP in solution. DEPA contains the P–N bond met in tabun. BAET possesses C–S and C–N bonds and imitates the big radical of VX attached to the phosphorus atom.

Experimental

Materials

Diethyl phosphoramidate (98%), dimethyl methylphosphonate ($\geq 97\%$), 2-(butylamino)ethanethiol, and pinacolyl methylphosphonate (97%) were supplied by Sigma-Aldrich and used without further purification. TiO₂ Hombikat UV 100 was supplied by Sachtleben Chemie GmbH. Deionized water was used for all experiments.

Trimethylsilyl (TMS) derivatization reagent *N,N*-bis(trimethylsilyl) trifluoroacetamide (BSTFA) + 1% trimethylchlorosilane (TMCS) was purchased from Supelco. The carbonyl group protection reagent *O*-methoxyamine was supplied from Supelco. Buffer with pH 7 containing 0.05 M solution of KH₂PO₄ and NaOH was a product of Fisher Scientific. Solid phase microextraction (SPME) was carried out using 85 μ m Carboxen/polydimethylsiloxane Stableflex fibers installed into a manual fiber holder, both supplied by Supelco.

Procedures and analyses

The sonophotocatalytic setup used for CWA simulants degradation is shown in Fig. 1. The cylindrical Pyrex reactor body carries a jacket for circulation of fluid from a thermostat. Oxygen was bubbled through a nozzle at the bottom of the reactor with a flow rate of 100 cm³ min⁻¹. Light from a 1000 W Xe lamp installed in an Oriel illuminator is directed to the top part of the reactor using a mirror. The flux of UV light entering the

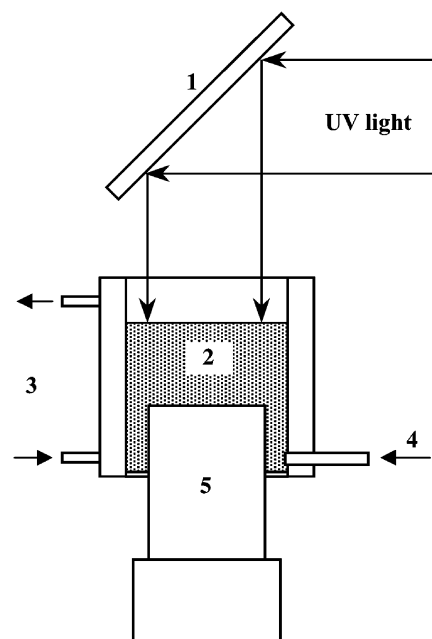


Fig. 1 Sonophotocatalytic setup: (1) mirror; (2) suspension of TiO₂ with CWA simulant; (3) inlet and outlet of water from a thermostat; (4) oxygen nozzle; (5) ultrasound transducer.

reactor was measured using ferrioxalate actinometry combined with a UV cutoff filter ($\lambda < 400$ nm) and was equal to 1.1×10^{-4} E s $^{-1}$. The suspension was sonicated using a 4.8 cm thick titanium horn powered by a 600 W GE 601 ultrasonic processor at 20 kHz. The amplitude of ultrasound was kept at 40% of maximum power, which corresponds to approximately 120 W of electric power. The power consumption was 40 W when the reactor was empty. Therefore, approximately 80 W was dissipated as ultrasound in the reaction mixture. The temperature inside the reactor was kept around 20 °C using a cooling thermostat.

For photocatalytic experiments, the ultrasound transducer at the bottom of the reactor was substituted with a Teflon bottom with a slightly different geometry. A magnetic stirrer provided agitation in this case.

Aqueous suspension of TiO $_2$ (250 mg l $^{-1}$) was prepared by stirring the mixture of TiO $_2$ and water for 20 min followed by sonication in an ultrasonic bath for 20 min and stirring again for 20 min. The appropriate amount of CWA simulant was added during the final stirring to lead to the required concentration of 250 mg l $^{-1}$.

After 200 ml of the suspension was poured into the reactor, ultrasound and/or ultraviolet irradiation was turned on and samples were taken using a syringe at various intervals. The total volume of suspension removed as samples did not exceed 25% of the initial suspension volume. TiO $_2$ was removed from samples by filtering through a 0.22 μ m Cameo polypropylene syringe filter. The samples were stored in a refrigerator at about 4 °C.

The pH measurements were done using a Fisher Accumet 25 pH meter with Accumet electrode. Necessary calibration was done before measurements using standard buffer solutions (Fisher Scientific).

The concentration of total carbon and inorganic carbon (IC) was measured using a Shimadzu TOC VCSH instrument. The concentration of total organic carbon (TOC) was determined from the difference between the concentration of total carbon and inorganic carbon.

Volatile products of degradation were analyzed either by direct injection into a Shimadzu QP5050A GC/MS instrument or using solid phase microextraction (SPME). Two and a half milliliters of sample was vigorously stirred in a 4 ml vial during SPME either with immersion of the fiber or using headspace absorption. Temperature of the samples was kept at about 25 °C during immersion SPME and about 60 °C during headspace absorption. Supelco Supel-Q PLOT column (30 m, 0.32 mm ID) was used for analysis of volatile products of CWA imitants destruction.

Non-volatile organic products were analyzed by means of substitution of active hydrogen atoms with the trimethylsilyl (TMS) group. The derivatization of products of DMMP, DEPA, and PMP degradation was successfully performed with samples evaporated to dryness in air. Two and a half milliliter samples in 4 ml vials were evaporated to dryness at approximately 60 °C. Then, 50 μ l of BSTFA + 1% TMCS reagent was added, and after at least 15 min the sample was analyzed using a Shimadzu XTI-5 column (30 m, 0.25 mm ID). Products of BAET degradation could not be analyzed with this method because evaporation of BAET samples, even at room temperature and in vacuum, resulted in dark residues insoluble in BSTFA + 1% TMCS reagent. Probably some products polymerized when the sample was concentrated. The strong acid H $_2$ SO $_4$ was detected in the BAET samples and could catalyze polymerization of products. For analyses of BAET samples, 2.5 ml of each sample was mixed with 0.25 ml of pH 7 phosphate buffer, 0.25 ml of 5 g l $^{-1}$ aqueous solution of *O*-methoxyamine, and slowly evaporated in air flow at 40–50 °C. In this procedure, carbonyl groups of products were protected by forming methoximes (MOX). The dry residue was dissolved in 50 μ l of BSTFA + 1% TMCS reagent. Some samples formed

a thick solution. An additional 150 μ l of BSTFA + 1% TMCS reagent provided almost complete dissolution of the thick samples. Successful analysis of DEPA-TMS derivatives required keeping the temperature of the GC/MS injection port and transfer line below 230 °C. To ensure detection of thermally unstable compounds, the temperature of the injection port and transfer line was kept at 200 °C.

Quantification of inorganic anions and cations was performed on a Dionex chromatograph with CD25 conductivity detector. The necessary calibrations were done for measurements of ion concentrations.

Identification of products

The mass spectra of products were searched in the NIST 98 library^{12a} and Wiley Registry of mass spectral data^{12b} (7th edition). The spectra were assigned to the corresponding products if they had at least 90% similarity to the corresponding library spectra. Mass spectra of a few products were absent from the mass spectra libraries. Their structure was suggested by using fragmentation patterns of recorded mass spectra in electron impact (EI) ionization mode.¹³ Methoxime derivatives usually had a [M–31] peak, TMS derivatives had *m/z* 73, multiple TMS derivatives with oxygen had *m/z* 147. Chemical ionization (CI) with methane as the reagent was applied to ascertain the molecular weight of all unknowns. The peak of the pseudo-molecular ion [M + 1] of TMS derivatives often had satellites at [M + 29], [M + 41], [M + 57], and [M + 73], which helped to determine the correct molecular weight (*M_w*).

The highest number of compounds absent from the libraries was met in MOX and TMS derivatized samples of BAET. The EI fragmentation patterns of major assigned and unassigned unknowns follow below.

C $_4$ H $_9$ NHCH $_2$ COOH + TMS, *M_w* 203: 15 (2.1%), 27 (7.3%), 28 (8%), 29 (13%), 30 (28%), 41 (8.9%), 42 (23%), 43 (7.9%), 44 (49%), 45 (11%), 47 (5%), 55 (13%), 56 (6.9%), 57 (6.7%), 61 (3.7%), 70 (3.9%), 72 (17%), 73 (13%), 75 (27%), 86 (100%), 87 (6.2%), 100 (3.1%), 103 (11%), 132 (1.9%), 156 (18%), 160 (6.6%), 188 (4%), 203 (3.3%).

C $_4$ H $_9$ NHCH $_2$ CHO + MOX + TMS, *M_w* 216: 15 (2%), 27 (4.8%), 29 (10%), 30 (2.5%), 31 (2.7%), 41 (6.9%), 42 (100%), 43 (11%), 44 (7.9%), 45 (20%), 56 (2.6%), 57 (6.1%), 58 (3.6%), 59 (19%), 69 (11%), 72 (4%), 73 (63%), 74 (7%), 86 (12%), 89 (14%), 100 (4.1%), 115 (3.8%), 116 (5%), 127 (2.3%), 144 (4.2%), 158 (5.8%), 168 (4.9%), 173 (22%), 174 (4.3%), 185 (19%), 186 (2.8%), 201 (1.9%), 216 (0.42%).

Unassigned *M_w* 305: 45 (9.3%), 59 (13%), 73 (50%), 86 (26%), 87 (2.6%), 89 (2.9%), 100 (13%), 114 (4.5%), 115 (3.8%), 130 (7.9%), 131 (2%), 144 (3.2%), 147 (2.2%), 158 (2%), 172 (2.8%), 174 (100%), 175 (19%), 176 (8.4%), 245 (2.43%), 248 (2.5%), 305 (0.59%).

C $_2$ H $_5$ C(O)CH $_2$ NHCH $_2$ COOH + MOX + 2 TMS, *M_w* 318: 29 (5.6%), 30 (2%), 41 (3.5%), 42 (91%), 43 (7.2%), 44 (4.5%), 45 (21%), 55 (2.9%), 56 (100%), 57 (5.9%), 58 (4.2%), 59 (15%), 69 (2.9%), 70 (7.8%), 73 (99%), 74 (9.2%), 75 (11%), 84 (2.7%), 86 (14%), 89 (3.3%), 97 (21%), 100 (15%), 101 (10%), 102 (4.9%), 103 (2.2%), 114 (18%), 115 (3%), 116 (3.3%), 120 (2.2%), 128 (4.9%), 129 (2.1%), 130 (3.1%), 133 (2.7%), 144 (2.7%), 147 (11%), 156 (6.1%), 163 (2%), 188 (1.6%), 201 (11%), 202 (8.3%), 203 (2.1%), 210 (5.7%), 216 (2%), 219 (2.4%), 232 (94%), 233 (18%), 234 (8%), 246 (3.1%), 287 (3.7%), 318 (6.7%).

C $_4$ H $_9$ NHCH $_2$ CH $_2$ SO $_2$ H + 2 TMS, *M_w* 309: 29 (3.4%), 41 (2.1%), 42 (4.8%), 43 (3%), 45 (12%), 56 (2.3%), 58 (2.2%), 59 (11%), 73 (100%), 74 (8.7%), 75 (8%), 86 (7.9%), 98 (4.2%), 100 (13%), 101 (8%), 104 (2.3%), 115 (15%), 116 (8.3%), 128 (9%), 129 (3.9%), 130 (3.7%), 147 (5%), 156 (39%), 157 (5.7%), 158 (20%), 160 (5.1%), 172 (73%), 173 (11%), 174 (3.5%), 209 (0.63%), 254 (1.2%), 266 (8.2%), 267 (1.7%), 268 (1.1%), 294 (1%).

$\text{CH}_3\text{CH}(\text{OH})\text{CH}_2\text{CH}_2\text{NHCH}_2\text{CH}_2\text{SO}_3\text{H} + 2 \text{ TMS}$, M_w 341: 45 (15%), 59 (16%), 73 (100%), 74 (8.9%), 75 (4.6%), 86 (6.4%), 100 (14%), 114 (4.1%), 130 (11%), 131 (4.3%), 133 (10%), 147 (48%), 148 (7.5%), 149 (3.9%), 160 (2.6%), 172 (4.9%), 174 (34%), 175 (6%), 176 (2.6%), 188 (19%), 189 (4%), 225 (7.1%), 238 (3.9%), 248 (2.9%), 326 (91%), 327 (26%), 328 (18%), 329 (3.9%).

$\text{C}_4\text{H}_9\text{NHCH}_2\text{CH}_2\text{SO}_3\text{H} + 2 \text{ TMS}$, M_w 325: 29 (4.9%), 41 (2.8%), 45 (11%), 55 (2.8%), 56 (26%), 57 (2.6%), 59 (9.5%), 73 (87%), 74 (7.7%), 75 (5.7%), 86 (5.9%), 87 (3.2%), 100 (2.5%), 101 (3.5%), 116 (4.4%), 133 (3.3%), 147 (14%), 158 (22%), 159 (3.2%), 172 (11%), 194 (2.7%), 225 (2.9%), 246 (2.2%), 253 (2.7%), 282 (100%), 283 (21%), 284 (14%), 285 (2.4%), 310 (7%), 325 (1.8%).

$(\text{C}_4\text{H}_9\text{NHCH}_2\text{CH}_2\text{S})_2$, M_w 264: 27 (3.4%), 29 (15%), 30 (26%), 41 (9.2%), 42 (4.6%), 43 (5.7%), 44 (34%), 56 (7.3%), 57 (9.2%), 58 (2.7%), 72 (3.5%), 73 (2.3%), 77 (2%), 84 (2.2%), 86 (100%), 87 (6.1%), 88 (6.1%), 89 (4.2%), 100 (25%), 101 (3.5%), 130 (2.2%), 132 (8.4%), 133 (20%), 134 (5.6%), 165 (25%), 166 (2.1%), 167 (2.2%).

Unassigned, M_w 360: 27 (2.9%), 29 (14%), 30 (12%), 42 (3.6%), 43 (3.3%), 44 (23%), 55 (2.2%), 56 (4.9%), 57 (9.3%), 86 (100%), 87 (7.6%), 88 (5.9%), 100 (3.6%), 132 (3%), 133 (2.1%), 140 (5.1%), 196 (1.2%), 228 (2.1%), 314 (6.9%).

Unassigned, M_w 456: 27 (4.1%), 29 (24%), 41 (23%), 42 (4.8%), 45 (2.7%), 55 (6%), 56 (4.4%), 57 (31%), 58 (2.3%), 59 (3.1%), 60 (2.4%), 61 (2.8%), 69 (3.1%), 88 (2%), 93 (2.1%), 126 (4.1%), 140 (60%), 141 (2.9%), 142 (0.27%), 165 (1.1%), 182 (1.8%), 196 (100%), 197 (9.3%), 228 (7.9%).

Unassigned, M_w 314: 27 (3.4%), 29 (15%), 30 (13%), 41 (10%), 42 (7.9%), 43 (7.9%), 44 (73%), 45 (9.3%), 47 (2.9%), 55 (2.3%), 56 (23%), 57 (27%), 58 (8.8%), 59 (3.2%), 70 (3.5%), 72 (4.7%), 73 (28%), 74 (3%), 75 (14%), 84 (16%), 86 (8%), 99 (3.4%), 100 (100%), 101 (7.4%), 104 (13%), 122 (3.5%), 137 (12%), 160 (1.5%), 194 (2.4%).

Results and discussion

Fig. 2 shows the change in total organic carbon (TOC) concentration during sonophotocatalytic degradation of the four chosen CWA simulants. The initial concentration of all the simulants was the same (250 mg l^{-1}) and the different initial concentrations of TOC reflects the different content of carbon atoms in the corresponding simulant molecules. Before switching on ultrasound and ultraviolet light, a blank run was carried out for 1 or 2 h for each simulant while bubbling O_2 through the suspension. No substantial change in TOC concentration was measured during the blank time, indicating negligible removal of simulants by evaporation. The initial concentrations of TOC for all the imitants are within experimental error of the theoretical concentrations: BAET, 135 mg l^{-1} ; DMMP, 73 mg l^{-1} ; DEPA, 79 mg l^{-1} ; and PMP, 117 mg l^{-1} . This indicates only weak adsorption of these molecules on the TiO_2 surface. The mean rates of TOC removal for all the compounds are summarized in Table 2. PMP showed the fastest rate of mineralization. The rates for other simulants were lower, the lowest rate being detected with BAET.

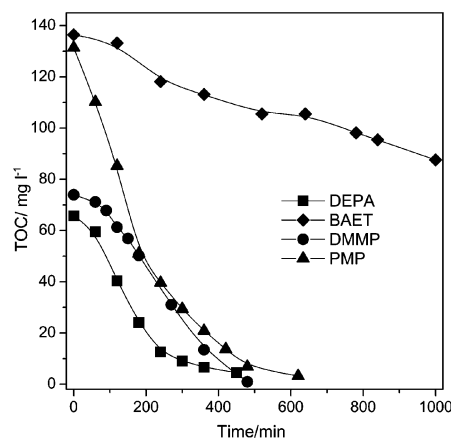


Fig. 2 TOC concentration as a function of time in sonophotocatalytic mineralization of CWA simulants.

Degradation of DMMP

Application of ultrasound increased the rate of TOC removal more than twofold in the case of DMMP (Table 2). One could suspect a synergistic effect of photocatalytic and ultrasonic treatments, as it was observed elsewhere.¹⁰ However, sonication of a TiO_2 suspension containing DMMP did not result in changes in either TOC or DMMP concentration (Fig. 3). O'Shea *et al.*⁵ also did not detect significant degradation of DMMP with ultrasound alone. Therefore, sonication itself does not destruct DMMP and the positive effect of ultrasound is seen only in combination with UV irradiation. Such an effect can be caused by (1) increased temperature and pressure at the microvoid implosion, (2) enhanced mass transport of reagents/products, (3) increase of the TiO_2 dispersion. TiO_2 Hombikat UV 100 contains micrometer size aggregates of primary particles of about 8 nm. Their partial deagglomeration with ultrasound increases the surface area available for reaction. Transport of reagents and products through nanometer-sized pores of TiO_2 agglomerates is slow in liquid phase and could be enhanced by ultrasound. Since ultrasound itself does not cause degradation of DMMP, we can expect the same products from sonophotocatalytic and photocatalytic degradation. The final and intermediate products residing in the solution were detected for DMMP photocatalytic degradation and are considered below. Fig. 4 shows changes of TOC, PO_4^{3-} concentration, and pH in DMMP photocatalytic oxidation. There is about a 2 h induction period in phosphate ion formation, which was also described in the paper by O'Shea *et al.*⁵ The pH value of the suspension decreased to about 3 and then almost levels though the concentration of phosphoric acid continued to increase. This may indicate that the increase in phosphoric acid concentration is balanced by decomposition of formic acid. Formic acid and formaldehyde are well known products of DMMP photocatalytic oxidation and were not sought in this work. They were detected and quantified in works by O'Shea *et al.*^{4,5} Methylphosphonic acid was also detected and quantified in their work. The overall mineraliza-

Table 2 Comparison of mean TOC removal and calculated oxygen consumption rate for sonophotocatalytic and photocatalytic degradation of CWA imitants

CWA imitant	TOC removal rate/ $\text{mg l}^{-1} \text{ min}^{-1}$		Oxygen consumption rate/ $\text{mg l}^{-1} \text{ min}^{-1}$	
	Sonophotocatalytic	Photocatalytic	Sonophotocatalytic	Photocatalytic
DMMP	0.17	0.062	0.22	0.080
DEPA	0.15	0.14	0.20	0.19
PMP	0.21	0.25	0.41	0.49
BAET	0.047	0.066	0.12	0.17

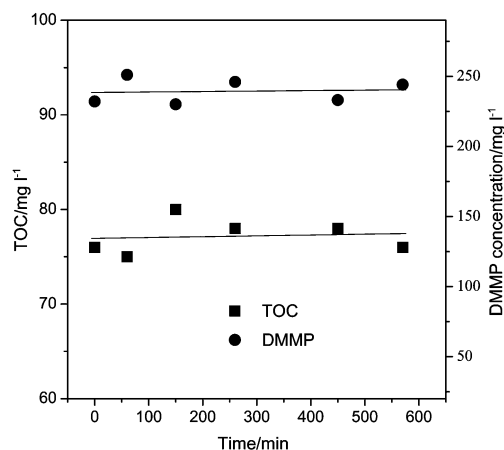


Fig. 3 TOC and DMMP concentration as a function of time during sonication of TiO₂ suspension containing DMMP.

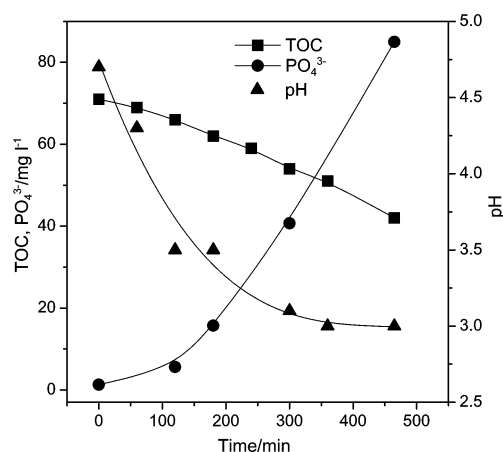
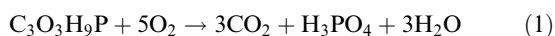


Fig. 4 Changes of TOC, phosphate concentration and pH during photocatalytic degradation of DMMP.

tion of DMMP proceeds according to the equation:



As in the works by O'Shea *et al.*, we could not detect methanol in the products. This contrasts to photocatalytic degradation of DMMP in the gas phase. Methanol formed, even in the dark, obviously *via* TiO₂ catalyzed hydrolysis.¹⁴ To estimate the impact of hydrolysis in our case, a TiO₂ suspension with DMMP was kept at room temperature for 23 days. The pH of the suspension only changed from 6.7 to 6.9 indicating the absence of hydrolysis. Non-volatile products of DMMP photocatalytic degradation were detected with GC/MS using TMS derivatization. The main products were methyl methylphosphonic acid (detected as mono-TMS ester), methylphosphonic acid (detected as di-TMS ester), and phosphoric acid (detected as tri-TMS ester). The other products that appeared in smaller quantities were: dimethylphosphoric acid (detected as mono-TMS ester), methylphosphoric acid (detected as di-TMS ester), dimethyl hydroxymethylphosphonic acid (detected as mono-TMS ester), methyl hydroxymethylphosphonic acid (detected as di-TMS ester), and hydroxymethylphosphonic acid (detected as tri-TMS ester). The latter products have not been reported previously. The observed set of products can be explained by consecutive oxidation of different CH₃ groups of the DMMP molecule. The proposed scheme of degradation is represented in Fig. 5. The reaction starts with oxidation of one of the methoxy groups or the methyl group. Oxidation of methoxy groups CH₃O-P of the DMMP molecule can result in HOCH₂O-P groups or, upon

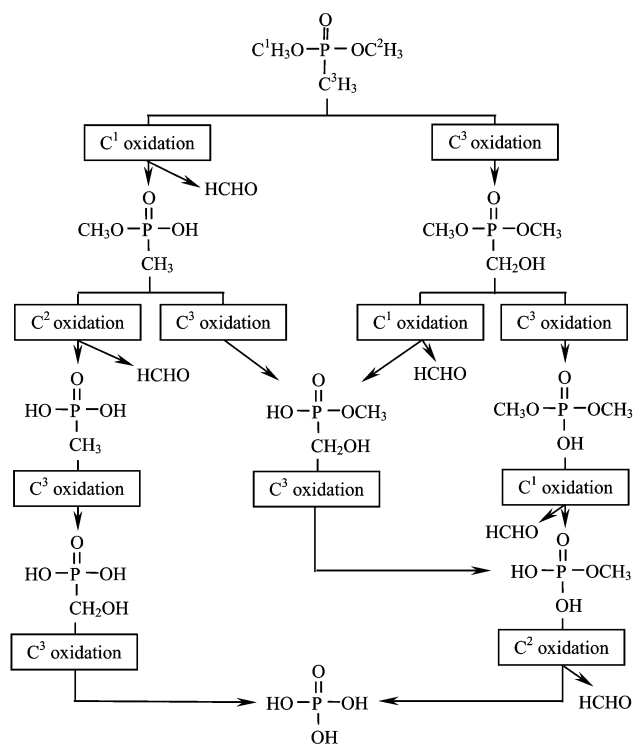
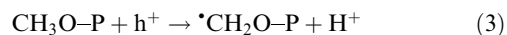
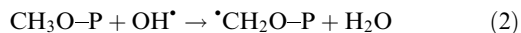


Fig. 5 Scheme of DMMP photocatalytic degradation. All shown products were detected.

further oxidation, in OCHO-P groups. The HOCH₂O-P group is a hemiacetal, which easily hydrolyzes in water to formaldehyde and the HO-P group and the hydrolysis rate increases when pH decreases.¹⁵ The OCHO-P group in DMMP represents an anhydride that quickly hydrolyzes in water to formic acid and the HO-P group. Oxidation of the methyl group CH₃-P leads to the HOCH₂-P group and the corresponding product, dimethyl hydroxymethylphosphonate, was detected. Further reactions represent combinations of oxidation of methoxy group and carbon attached directly to phosphorus. The possible products of the latter reaction containing OHC-P and HOOC-P groups should be stable in water but were not detected in the products. It is possible that they are quickly oxidized, resulting in HO-P group. The products in the left part of Fig. 5 prevail. Therefore, the main route of DMMP photocatalytic oxidation is oxidation of methoxy groups followed by oxidation of the methyl group.

Below we will consider possible mechanisms of the oxidative reactions involved in DMMP degradation. Hydroxyl radicals OH[•] and photogenerated holes h⁺ in the valance band of TiO₂ are considered as species conducting oxidative reactions at the surface of TiO₂ particles. It is often difficult to choose which species, OH[•] or h⁺, carries out the oxidation. This is also the case for oxidation of the methoxy groups of DMMP. Attack by both hydroxyl radicals and holes



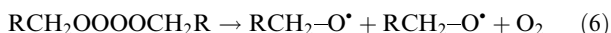
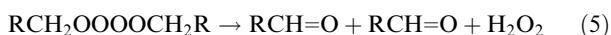
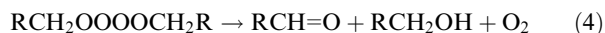
will produce the same radical that can undergo further transformations discussed below.

However, oxidation of the methyl group CH₃-P can be started only by reaction with OH[•] radicals because reaction of DMMP with holes would proceed at methoxy groups.

Further transformations of [•]CH₂O-P and [•]CH₂-P radicals can proceed *via* diffusion limited reactions with OH[•] radical to form HOCH₂O-P and HOCH₂-P or with oxygen to form peroxy radicals [•]OOCH₂O-P and [•]OOCH₂-P. Hydroxyl radicals are very active species tending to recombine or scavenge H

atoms from organics and therefore their concentration is very low. The concentration of oxygen in aqueous solution is of the order of 1 mM. Thus, reaction with oxygen is more probable.

Peroxyl radicals can undergo unimolecular and bimolecular transformations.¹⁶ Unimolecular processes comprise HO_2^\bullet elimination (if a double bond is formed), O_2^\bullet elimination, addition to the C=C double bond, hydrogen abstraction (both intra- and intermolecular). The bimolecular processes are electron transfer, oxygen transfer, and recombination to form intermediate tetroxide ROOOOR . The tetroxide is very unstable at room temperature due to the low energy of the middle O–O bond ($21\text{--}33\text{ kJ mol}^{-1}$) and decomposes *via* the following four competitive channels:¹⁶



If we follow the arguments and experimental information presented by von Sonntag and Schuchmann,¹⁶ transformation of the peroxyl radicals $^\bullet\text{OOCH}_2\text{O-P}$ and $^\bullet\text{OOCH}_2\text{-P}$ should proceed mostly *via* tetroxide intermediates with domination of the products of channels (4) and (5) of their decay. This means formation of OCH-O-P , $\text{HOCH}_2\text{O-P}$ for peroxyl radical $^\bullet\text{OOCH}_2\text{O-P}$, and OCH-P , $\text{HOCH}_2\text{-P}$ for peroxyl radical $^\bullet\text{OOCH}_2\text{-P}$. As we considered above, OCH-O-P and $\text{HOCH}_2\text{O-P}$ form the detected products HCOOH , HCHO , and HO-P in water. Products containing $\text{HOCH}_2\text{-P}$ group were also detected, and only OCH-P group was not detected. Thus, photocatalytic degradation of DMMP can be successfully explained by reactions of peroxyl radicals. Further oxidation of $\text{HOCH}_2\text{-P}$ and OHC-P groups can go via reactions with OH^\bullet radicals and/or holes h^+ . The possible intermediate group HOOC-P can be transformed into CO_2 and a trivalent phosphorus group *via* the Kolbe reaction. The trivalent phosphorus group should be converted into HO-P(V) by reaction with holes and water.

Photocatalytic degradation of DEPA

DEPA contains the P–N bond that is present in tabun (GA) and can provide an estimate for the ability of TiO_2 photocatalysis to detoxify tabun. Fig. 6 shows concentration *versus* time dependence for TOC and inorganic ions. The initial concentration of DEPA is 1.63 mM. Almost all the organic carbon in the solution is converted into inorganic species after 540 min of reaction. The concentration of NO_3^- and NH_4^+ ions after 540 min of reaction totals 1.6 mM, and the concentration of

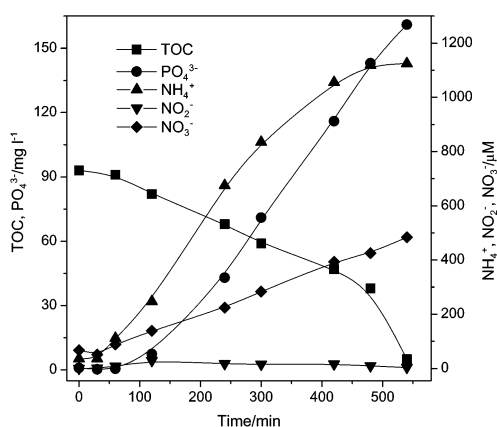
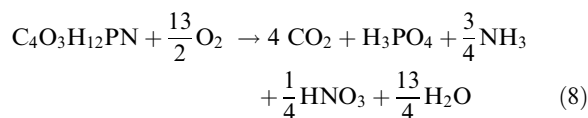


Fig. 6 TOC and inorganic ions concentration as a function of time during photocatalytic degradation of DEPA.

PO_4^{3-} also corresponds to complete mineralization of all the DEPA. This indicates that no significant quantity of unreacted DEPA resides on the surface of TiO_2 . The complete mineralization of DEPA follows the reaction:



After 400 min of reaction, the concentration of NH_4^+ starts to level off, whereas the concentration of NO_3^- continues to grow. This indicates that part of the generated NH_4^+ ions may be converted into NO_3^- ions. NO_2^- ions are considered as an intermediate in the formation of NO_3^- ions and their concentration does not exceed $1.4\text{ }\mu\text{M}$. The higher yield of ammonia compared to nitrate is usual for the degradation of organic compounds containing nitrogen in oxidation state -3 .^{9,17,18} Piccinini *et al.*¹⁸ observed predominate formation of NH_4^+ ions even during degradation of organic compounds with nitrogen in oxidation state $+1$. They also observed interconversion of NO_3^- and NH_4^+ species in illuminated TiO_2 suspensions. Therefore, photocatalytic degradation in oxygenated water suspensions can lead to reduction of species.

As in the case of DMMP, we did not detect alcohol as a product of degradation. Single ion monitoring and SPME was used to detect small amount of ethanol that could be formed as a product. However, a very small concentration of ethanol present initially in the suspension as impurity became even smaller after the reaction started. Volatile products detected by SPME are acetaldehyde and acetic acid. Several non-volatile products were detected after derivatization. The detected products are listed in Table 3. The major products are diethylphosphoric acid and ethylphosphoric acid. Hydroxyacetic acid, 2-hydroxyethyl ethylphosphoric acid, 2-hydroxyethyl ethylphosphoramidate, ethylphosphoramidate, and bis(2-hydroxyethyl)phosphoric acid were detected in smaller quantities. It was not possible to provide calibrations for all the organic compounds encountered in this study. Nevertheless, qualitative information about the concentration profiles of products can be useful for confirming which compounds are intermediates and understanding kinetics.

Fig. 7 shows qualitative profiles of concentrations of organic products during DEPA photocatalytic degradation. The curves were obtained by normalizing the area of the chromatographic peaks for selected ions to the maximum area for each organic compound. Concentration of DEPA in Fig. 7 is the sum of the concentrations of mono-TMS and di-TMS derivatives of DEPA. The DEPA concentration falls to zero after 420 min of reaction. Therefore, all TOC in the suspension after 420 min of reaction is associated with reaction products. One can observe in Fig. 6 that TOC concentration decreases much faster after 420 min of reaction. The explanation is that the products of DEPA degradation are easier to degrade to inorganic products than the starting molecule. The profile of phosphate ions is plotted in Fig. 7 to check whether analysis by trimethylsilylation allows us to obtain adequate qualitative profiles of the concentration. When comparing the PO_4^{3-} profile in Fig. 7 to that in Fig. 6, one can see that the shape of the curves is similar and the curves have the same induction period of about 100 min. The profiles of almost all other products also have an induction period. We believe that this behavior is at least partially associated with the hydrolysis rate of intermediates. Initially, the pH of the solution is close to 7, but it becomes acidic during the reaction. Acids produced in DEPA degradation catalyze the hydrolysis reactions. It is interesting to note in Fig. 7 that concentrations of diethyl phosphate and ethyl phosphate increase and decrease almost simultaneously although ethyl phosphate should be formed from diethyl phosphate.

Table 3 Detected products of DEPA photocatalytic degradation

Measured by ion chromatography	Detected by trimethylsilylation	Detected by immersion SPME
PO_4^{3-}	$\begin{array}{c} \text{O} \\ \parallel \\ \text{C}_2\text{H}_5\text{O}-\text{P}-\text{OC}_2\text{H}_5 \\ \\ \text{OH} \end{array}$ (Diethylphosphate)	CH_3CHO (Acetaldehyde)
NH_4^+ NO_2^-	$\begin{array}{c} \text{O} \\ \parallel \\ \text{C}_2\text{H}_5\text{O}-\text{P}-\text{OH} \\ \\ \text{OH} \end{array}$ (Ethylphosphate) HOCH_2COOH (Hydroxyacetic acid)	CH_3COOH (Acetic acid)
NO_3^-	$\begin{array}{c} \text{O} \\ \parallel \\ \text{C}_2\text{H}_5\text{O}-\text{P}-\text{OCH}_2\text{CH}_2\text{OH} \\ \\ \text{OH} \end{array}$ (2-Hydroxyethyl ethylphosphoric acid) $\begin{array}{c} \text{O} \\ \parallel \\ \text{C}_2\text{H}_5\text{O}-\text{P}-\text{OCH}_2\text{CH}_2\text{OH} \\ \\ \text{NH}_2 \end{array}$ (2-Hydroxyethyl ethylphosphoramidate) $\begin{array}{c} \text{O} \\ \parallel \\ \text{C}_2\text{H}_5\text{O}-\text{P}-\text{OH} \\ \\ \text{NH}_2 \end{array}$ (Ethylphosphoramidate) $\begin{array}{c} \text{O} \\ \parallel \\ \text{OH}-\text{CH}_2-\text{P}-\text{CH}_2-\text{OH} \\ \\ \text{OH} \end{array}$ [Bis(2-hydroxyethyl)phosphoric acid]	

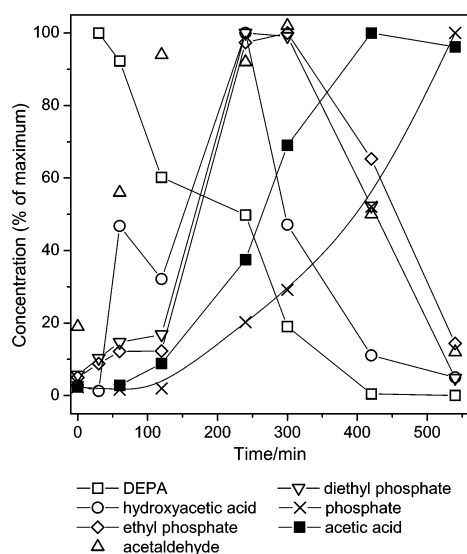
**Fig. 7** Normalized concentration of products of DEPA photocatalytic degradation detected using trimethylsilylation and SPME.

Fig. 8 shows the scheme of DEPA photocatalytic degradation. The reaction starts with cleavage of the N–P bond and oxidation of the α and β carbon atoms of the ethoxy groups, cleavage of the N–P bond being the dominant reaction. The further dominant route is oxidation of the α carbon of ethoxy groups. Other further transformations comprise combinations of N–P bond cleavage, and oxidation of α and β carbon atoms. Similarly to photocatalytic destruction of DMMP, oxidation at carbon atoms is expected to result in hydroxyl and carbonyl groups. Thus, oxidation of α carbon atoms of ethoxy group would produce $\text{P}-\text{CH}(\text{OH})\text{CH}_3$ and

$\text{P}-\text{C}(\text{O})\text{CH}_3$, both subject to hydrolysis into detected acetaldehyde and acetic acid, respectively. Oxidation of the β carbon of ethoxy groups should produce $\text{P}-\text{OCH}_2\text{CH}_2\text{OH}$ and $\text{P}-\text{OCH}_2\text{CHO}$, as well as $\text{P}-\text{OCH}_2\text{COOH}$, all being stable in water. The first group was detected in small quantities while the latter two were not detected, probably because of their high reactivity.

Oxidation of α carbon atoms can be started either by hydroxyl radicals or by valence band holes in TiO_2 . Only hydroxyl radicals can start oxidation of β carbon atoms. The predominance of oxidation of α carbon atoms, however, does not prove that reaction with holes is the main process, because abstraction of hydrogen from the α carbon atom of ethoxy groups by hydroxyl radicals is much faster than that from β carbon atoms.¹⁹ The further mechanism of alkyl radical transformation is supposed to be similar to that of DMMP. Peroxyl radicals from reaction with oxygen recombine and mainly follow reactions (4) and (5) to produce corresponding hydroxyl and carbonyl groups.

Photocatalytic degradation of PMP

Pinacolyl methylphosphonic acid (PMP) has a structure identical to soman (GD) except that a hydroxyl group replaces the fluorine atom of soman. PMP is the hydrolysis product of soman. Though the toxicity of PMP is low, it is important to destroy it since soman can be obtained from PMP, whereas one will require irreversible destruction of all the CWA.

Fig. 9 shows the absolute concentration of TOC and phosphate ions as well as concentration in arbitrary units of PMP and methylphosphonic acid (MP) during photocatalytic degradation of PMP. The concentration of PMP decreases to almost zero after 200 min of reaction but TOC concentration approaches zero only in 480 min of reaction and the phosphate ion concentration reaches the stoichiometric value at this time. Therefore, the longest process is to mineralize the organic

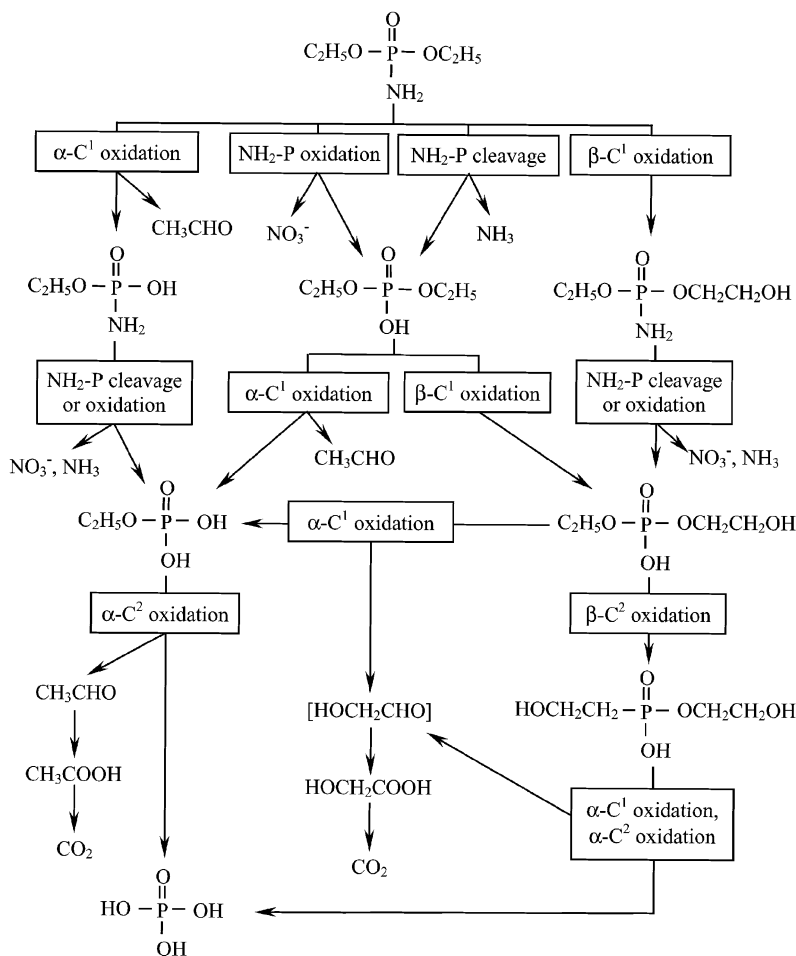


Fig. 8 Scheme of DEPA photocatalytic degradation. C¹ corresponds to carbon atoms in the ethoxy group that is oxidized first, C² corresponds to those in the ethoxy group oxidized second. Compound in brackets was not detected.

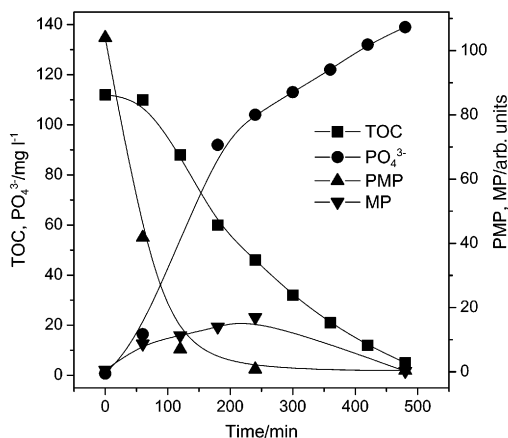
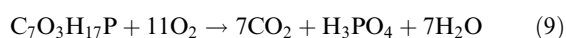


Fig. 9 Profiles of TOC and phosphate concentration as well as normalized concentration of PMP and methylphosphonic acid (MP) in photocatalytic degradation of PMP.

products of PMP degradation. The complete mineralization of PMP follows the reaction:



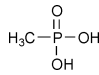
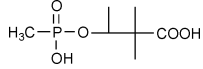
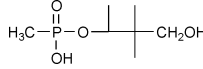
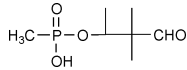
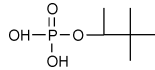
In contrast to the photocatalytic degradation of DMMP and DEPA, which resulted in few volatile products, the photocatalytic degradation of PMP produced about a dozen volatile organic products. They were detected by SPME and are listed in the third column of Table 4. The major volatile product is acetone; other products were detected in much smaller quanti-

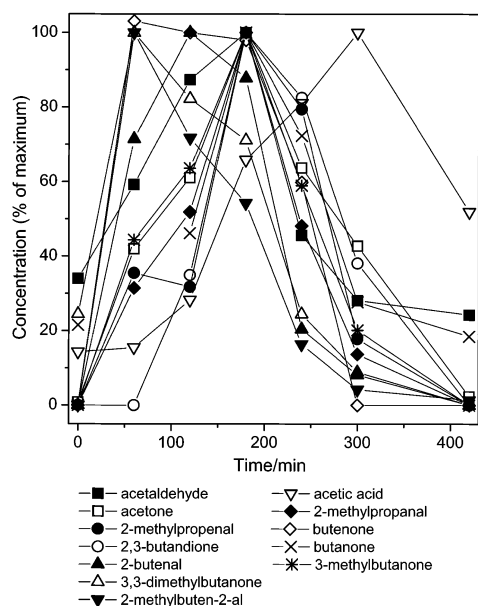
ties. Normalized profiles of their concentrations are represented in Fig. 10. The time at which peaks of concentration profiles appear may indicate how quickly compounds appear in the PMP degradation mechanism. Three compounds have their peak concentrations at the earliest time of reaction: 2-methylbutenal-2, 3,3-dimethylbutanone, and butanone. The next is the peak of 2-butenal, and then all other compounds follow except acetic acid, which has the latest peak.

Several non-volatile products of PMP photocatalytic degradation were detected after trimethylsilylation (column 2 in Table 4). The main product was methylphosphonic acid; the products in smaller concentrations were 1,2-dimethyl-2-formylpropyl methylphosphonic acid, 3-hydroxy-1,2,2-trimethylpropyl methylphosphonic acid, 2-carboxy-1,2-dimethylpropyl methylphosphonic acid, and pinacolylphosphoric acid. Non-phosphorous products were hydroxyacetic acid, 2-hydroxypropanoic acid, ethylpropanedioic acid, and 2-methyl-2-hydroxypropanoic acid. Dibasic acid, alcohol and aldehyde derivatives of PMP not listed in Table 4 were also suggested, mainly on the basis of the molecular weights of product chromatographic peaks.

The pinacolyl fragment of PMP molecule is more complex than the alkoxyl fragments of DMMP and DEPA. The variety of volatile products of PMP degradation suggests a complex mechanism with many possibilities for crossing and branching pathways. Because of this complexity the complete pathways of degradation are not suggested. However, we can draw the scheme for how the degradation of PMP gets started (Fig. 11). The set of detected products suggests that oxidation starts mainly at three structurally different carbon centers: CH₃-P group, α carbon of pinacolyl, and γ carbons of

Table 4 Main detected products of PMP photocatalytic degradation

Measured by ion chromatography	Detected by trimethylsilylation	Detected by immersion SPME
PO_4^{3-}		CH_3COCH_3 (Acetone)
	(Methylphosphonic acid)	CH_3COOH (Acetic acid) $\text{CH}_3\text{CH}=\text{C}(\text{CH}_3)\text{CHO}$ (2-Methylbutenal-2)
		(CH_3) ₂ CHC(O)CH ₃ CHC(O)CH ₃ (3-Methylbutanone) CH_3CHO (Acetaldehyde)
	(2-Carboxy-1,2-dimethylpropyl methylphosphonic acid)	
		$\text{CH}_2=\text{C}(\text{CH}_3)\text{CHO}$ (2-Methylpropenal) $\text{CH}_3\text{CH}_2\text{C}(\text{O})\text{CH}_3$ (Butanone) $\text{CH}_3\text{C}(\text{O})\text{C}(\text{O})\text{CH}_3$ (Butandione)
	(3-Hydroxy-1,2,2-trimethylpropyl methylphosphonic acid)	
		$\text{CH}_3\text{CH}(\text{CH}_3)\text{CHO}$ (2-Methylpropanal) $\text{CH}_3\text{CH}=\text{CHCHO}$ (Propenal-2)
	(1,2-Dimethyl-2-formylpropyl methylphosphonic acid)	
		(CH_3) ₃ CC(O)CH ₃ (3,3-Dimethylbutanone) $\text{CH}_2=\text{CHC}(\text{O})\text{CH}_3$ (Butenone)
	(Pinacolylphosphoric acid)	
	HOCH_2COOH (Hydroxyacetic acid)	
	$\text{CH}_3\text{CH}(\text{OH})\text{COOH}$ (2-Hydroxypropanoic acid)	
	$\text{CH}_3\text{CH}_2\text{CH}(\text{COOH})\text{COOH}$ (Ethylpropanedioic acid)	
	$\text{CH}_3\text{C}(\text{CH}_3)(\text{OH})\text{COOH}$ (2-Methyl-2-hydroxypropanoic acid)	

**Fig. 10** Normalized concentration of organic intermediates in PMP photocatalytic degradation as determined by immersion SPME.

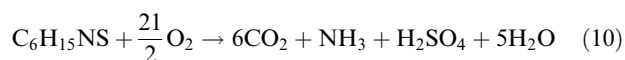
pinacolyl. Oxidation of the $\text{CH}_3\text{-P}$ group results in a HO-P group and the possible alcoholic intermediate was not detected. Oxidation at α carbon of pinacolyl could result in introduction of an α hydroxyl group, a structure equivalent to a hemiacetal. It hydrolyzes in water to form detected methylphosphonic acid and 3,3-dimethylbutanone. Oxidation at γ carbons of pinacolyl results in γ hydroxyl, carbonyl and carboxyl groups.

It seems the oxidation starts mostly *via* reaction of PMP with hydroxyl radicals since valence band holes of TiO_2 can

only start oxidation at the α carbon of pinacolyl. Oxidation of the pinacolyl fragment proceeds most probably *via* formation and reactions of peroxy radicals. The stages of this mechanism were considered in the DMMP degradation section.

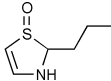
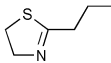
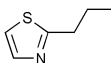
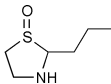
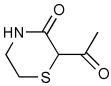
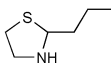
Photocatalytic degradation of BAET

2-(Butylamino)ethanethiol (BAET) imitates the sulfur and nitrogen containing radical of VX. It also imitates the product of P-S bond cleavage in VX. The profiles of TOC and inorganic ion concentrations are plotted in Fig. 12 for BAET photocatalytic degradation. One can observe that a 660 min reaction time resulted in only 29% conversion of TOC. However, the concentration of sulfate ions after 660 min reached 118 ppm, which corresponds to 66% conversion of all the sulfur in solution. The concentration of nitrite and nitrate ions changed negligibly during the reaction. The main final nitrogen species is ammonia, whose concentration at 600 min of reaction is 390 μM , or 21% of initial nitrogen of BAET. The BAET mineralization follows the reaction:



A wide variety of volatile and non-volatile products were detected in samples from BAET photocatalytic degradation. Identification of unknown compounds in this case was more difficult than for previously considered imitants because there were many variants and isomers that could correspond to the same molecular weight product. Therefore, compounds that were identified without comparing to library mass spectra are marked as “suggested” in Table 5, and the molecular weight (M_w) is given for these compounds. The main volatile products of BAET degradation are butanal and a compound with M_w 145, which was attributed to 2-propyldihydrothiazole-S-oxide. Other prominent chromatographic peaks corre-

Table 5 Main detected products of BAET photocatalytic degradation

Measured by ion chromatography	Detected by trimethylsilylation	Detected by headspace SPME and direct injection
SO_4^{2-}	$\text{NH}_2\text{CH}_2\text{COOH}$ (Glycine) $\text{CH}_3(\text{C}_2\text{H}_3\text{OH})\text{COOH}$ (2- or 3-Hydroxybutanoic acid)	$\text{CH}_3\text{CH}_2\text{CH}_2\text{CHO}$ (butanal)  (2-Propyldihydrothiazole- <i>S</i> -oxide) (suggested for M_w 145) $\text{CH}_2=\text{CHC}(\text{O})\text{CH}_3$ (Methylvinylketone) $\text{CH}_3\text{CH}=\text{CHCHO}$ (2-Butenal) $\text{CH}_3\text{CH}_2\text{CH}_2\text{CN}$ (Cyanopropane) $\text{CH}_3\text{CH}_2\text{CHO}$ (Propanal)
NH_4^+	$\text{CH}_3\text{CH}_2\text{CH}_2\text{CH}_2\text{NH}_2$ (<i>n</i> -Butylamine) H_2SO_4 (Sulfuric acid)	CH_3CHO (Acetaldehyde)  (2-Propylthiazoline)  (2-Ethyl-1,4-thiazine) (suggested for M_w 129)
NO_3^-	$\text{C}_4\text{H}_9\text{NHCH}_2\text{COOH} + \text{TMS}$ [2-(<i>N</i> -Butylamino)acetic acid] (suggested for M_w 203)	$\text{CH}_3\text{CH}(\text{O})\text{CH}_2\text{CH}_2\text{NHCH}_2\text{COOH} + \text{MOX} + \text{TMS}$ (2-Oxobutylaminoacetic acid) (suggested for M_w 318)
NO_2^-	$\text{C}_4\text{H}_9\text{NHCH}_2\text{CHO} + \text{MOX} + \text{TMS}$ [2-(<i>N</i> -Butylamino)acetaldehyde] (suggested for M_w 216) $\text{NH}_2\text{CH}_2\text{CH}_2\text{OH} + 2\text{TMS}$ (Aminoethanol) $\text{C}_4\text{H}_9\text{NHCH}_2\text{CH}_2\text{SO}_2\text{H} + 2\text{TMS}$ [2-(Butylamino)-ethanesulfonic acid] (suggested for M_w 309) $\text{CH}_3\text{CH}(\text{OH})\text{CH}_2\text{CH}_2\text{NHCH}_2\text{CH}_2\text{SO}_3\text{H} + 2\text{TMS}$ [2-(3-Hydroxybutylamino)ethanesulfonic acid] (suggested for M_w 325)	 (thiirane)  (2-Propylthiazole) CS_2  (pyrrole) $\text{CH}_2=\text{CHCHO}$ (Acrolein) $\text{CH}_3\text{CH}_2\text{CH}_2\text{CH}_2\text{NO}_2$ (Nitrobutane) $\text{CH}_3\text{CH}_2\text{CH}_2\text{CH}_2\text{SCN}$ (Butylthiocyanide) CH_3COOH (Acetic acid)  (2-Propylthiazolidinesulfoxide) (suggested for M_w 163)  (2-Acylthiazine-3-on) (suggested for M_w 159)  (2-Propylthiazolidine)
	M_w 360 (Structure not suggested)	
	M_w 456 (Structure not suggested)	
	M_w 314 (Structure not suggested) M_w 305 (Structure not suggested)	

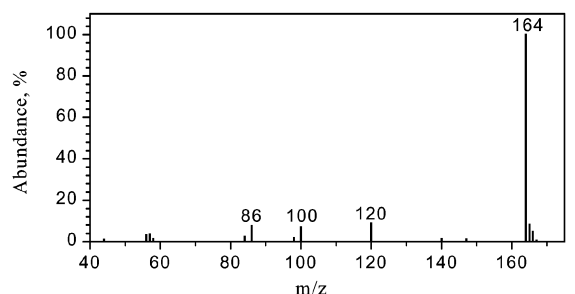
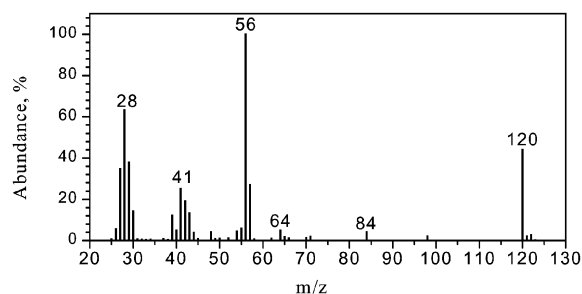
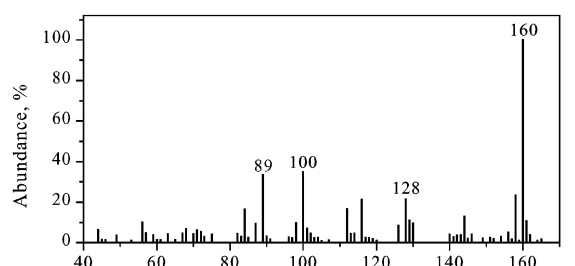
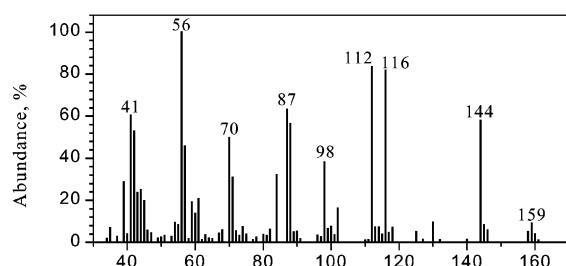
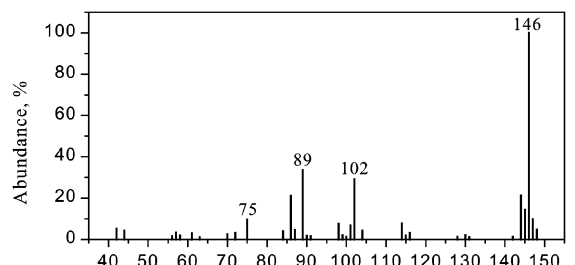
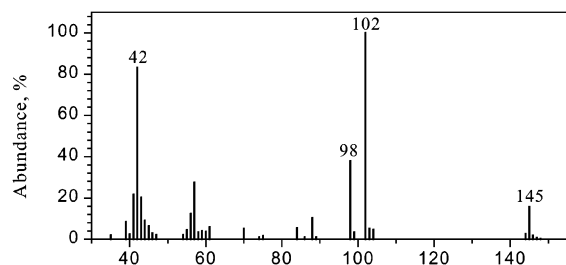
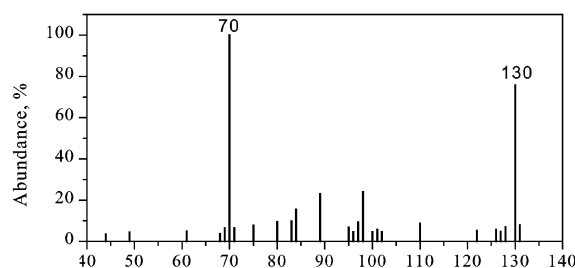
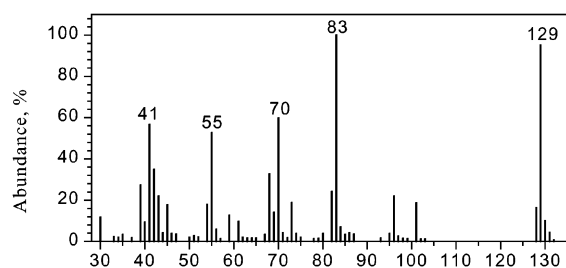


Fig. 13 Electron impact (left) and chemical ionization (right) mass spectra of several products of BAET photocatalytic degradation.

pared in Table 2. Ultrasonic irradiation induced a significant acceleration of photocatalytic degradation for DMMP. The rates for other CWA imitants are approximately the same with and without sonication. This result is not surprising because sonochemical and sonophotocatalytic degradation are known to be sensitive to conditions and type of substrate. For example, the rate of sonophotocatalytic degradation of trichlorophenol was lower than the rate of photocatalytic degradation at 30 °C and higher at 45 °C.²² Sonochemical and sonophotocatalytic degradation are thought to depend on the distribution of substrate between solution and the gas–solution interphase of cavitation bubbles. We used very different substrates and can expect different distributions of them between solution and the gas–solution interface.

Assuming that one photon is necessary to mineralize each molecule of CWA imitant, the quantum efficiency for complete photocatalytic mineralization of imitants was estimated as 0.0015% for DMMP, 0.0028% for DEPA, 0.004% for PMP, and 0.0015% for BAET.

Conclusions

Complete mineralization of compounds imitating chemical warfare agents, namely dimethyl methylphosphonate (DMMP), diethylphosphoramidate (DEPA) and pinacolyl methylphosphonate (PMP), was achieved in suspensions of TiO₂ with simultaneous ultrasonication and ultraviolet irradiation as well as with ultraviolet irradiation alone. 2-Butylaminoethanethiol (BAET) also converted to inorganic products but required a longer time for the same mass. Comparison of sonophotocatalytic and photocatalytic treatment showed acceleration of mineralization by sonication for DMMP. Volatile and non-volatile organic products as well as inorganic ions were detected and monitored during the photocatalytic degradation. Degradation of phosphorous-containing organics was always finalized by phosphate ions, organic sulfur converted into sulfate ions, but nitrogen converted to nitrate ions (25%) and ammonia (75%) in the case of DEPA, and to ammonia only in the case of BAET. Pathways of degradation were

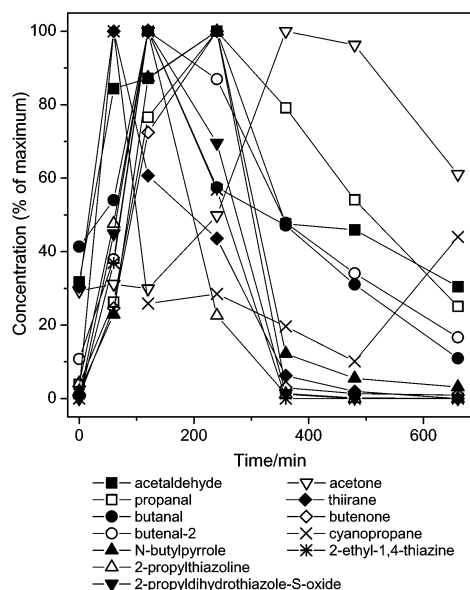


Fig. 14 Changes in normalized concentration of main organic products of BAET photocatalytic degradation as detected by headspace SPME.

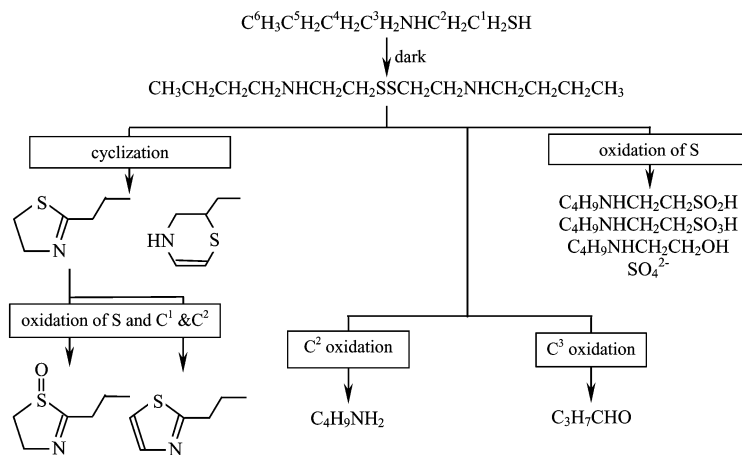


Fig. 15 Main starting routes of BAET photocatalytic degradation.

proposed for DMMP and DEPA and starting routes for PMP and BAET. The results demonstrate the feasibility of photocatalysis for destruction of chemical warfare agents in aqueous phase. Optimization of degradation conditions is necessary to achieve practical quantum efficiencies.

Acknowledgements

We gratefully acknowledge the support of the US Department of Army Young Investigator Program under grant no. DAAD 19-00-1-0399, and NATO Science for Peace Programme grant SfP 974209. We also acknowledge funding from the Ohio Board of Regents (OBR) that provided matching funds for equipment to the NSF CTS-9619392 grant through the OBR Action Fund #333. We would like to thank Prof. D. D. Dionysiou and Mr G. Anipsitakis for the help with ion chromatographic measurements.

References

- Y.-C. Yang, *Chem. Ind.*, 1995, **9**, 334.
- Y.-C. Yang, J. A. Baker and J. R. Ward, *Chem. Rev.*, 1992, **92**, 1729.
- C. Lion, L. Da Conceição, G. Magnaud, G. Delmas and M. Desgranges, *Rev. Sci. Tech. Def.*, 2001, **52**, 139.
- K. E. O'Shea, S. Beightol, I. Garcia, M. Aguilar, D. V. Kalen and W. J. Cooper, *J. Photochem. Photobiol., A*, 1997, **107**, 221.
- K. E. O'Shea, I. Garcia and M. Aguilar, *Res. Chem. Intermed.*, 1997, **23**, 325.
- T. N. Obee and S. Satyapal, *J. Photochem. Photobiol., A*, 1998, **118**, 45.
- R. Doong and W. Chang, *J. Photochem. Photobiol., A*, 1997, **107**, 239.
- M.-C. Lu, G.-D. Roam, J.-N. Chen and C. P. Huang, *Chem. Eng. Commun.*, 1995, **139**, 1.
- G. Liu and J. Zhao, *New J. Chem.*, 2000, **24**, 411.
- A. J. Johnston and P. Hocking, *ACS Symp. Ser.*, 1993, **518**, 106.
- A. V. Vorontsov, E. N. Savinov, L. Davydov and P. G. Smirniotis, *Appl. Catal., B*, 2001, **32**, 11.
- (a) NIST/EPA/NIH Mass Spectral Database, National Institute of Standards and Technology, Gaithersburg, MD, 1998; (b) F. McLafferty, *Wiley Registry of Mass Spectral Data*, CD-ROM, Wiley, New York, 7th edn., 2000.
- F. W. McLafferty, *Interpretation of Mass Spectra*, W. A. Benjamin, Inc., Reading, MA, 1973.
- C. N. Rusu and J. T. Yates, *J. Phys. Chem. B*, 2000, **104**, 12 299.
- J. Clayden, N. Greeves, S. Warren and P. Wothers, *Organic Chemistry*, Oxford University Press, Oxford, New York, 2001.
- C. von Sonntag and H.-P. Schuchmann, in *Peroxy Radicals*, ed. Z. Alfassi, Wiley, Chichester, England, p. 173.
- S. Horikoshi, N. Watanabe, M. Mukae, H. Hidaka and N. Serpone, *New J. Chem.*, 2001, **25**, 999.
- P. Piccinini, C. Minero, M. Vincenti and E. Pelizzetti, *Catal. Today*, 1997, **39**, 187.
- P. Neeb, *J. Atmos. Chem.*, 2000, **35**, 295.
- D. K. Rohrbaugh, *J. Chromatogr. A*, 1998, **809**, 131.
- T. Cassagne, H.-J. Cristau, G. Delmas, M. Desgranges, C. Lion, G. Magnaud, E. Torrelles and D. Virieux, *C. R. Acad. Sci., Ser. IIc: Chim.*, 2001, **4**, 309.
- I. Z. Shiraonkar and A. B. Pandit, *Ultrason. Sonochem.*, 1998, **5**, 53.